Title
Thin (actin) and thick (myosinlike) filaments in cone contraction in the teleost retina.

THIN (ACTIN) AND THICK (MYOSINLIKE) FILAMENTS

IN CONE CONTRACTION IN THE TELEOST RETINA

BETH BURNSIDE

From the Bermuda Biological Station for Research, St. George, Bermuda, and the Department of Physiology-Anatomy, University of California, Berkeley, California 94720

ABSTRACT

The long slender retinal cones of fishes shorten in the light and elongate in the dark. Light-induced cone shortening provides a useful model for studying nonmuscle contraction because it is linear, slow, and repetitive. Cone cells contain both thin (actin) and thick (myosinlike) filaments oriented parallel to the axis of contraction. This study examines the polarities of the cone's thin filaments and the changes in filament distribution which accompany light-induced contraction, in an attempt to elucidate the structural basis for the cone's contractile process.

The proximal half of the cone is fixed to its cellular neighbors in the outer nuclear layer while the distal half is free. Thus, all shortening takes place in a necklike region (the myoid) in the distal half of the cone which extends into the space between the neural retina and the pigmented retinal epithelium. Thin filaments are found throughout the length of the cone, whereas thick filaments occur predominantly in the proximal (axon) regions of both light- and dark-adapted cones. Thus, thick filaments are primarily localized outside the region where shortening takes place.

Observations from myosin subfragment-1 binding studies suggest that the cone's thin filaments are organized into two opposing sets. In the distal half of the cone (including the myoid), virtually all filaments have proximally directed arrowheads. In the more proximal regions of the axon, many thin filaments have opposite polarity, their arrowheads being distally directed. Near the synaptic proximal end of the light-adapted (contracted) cone, filaments of opposite polarities occur in approximately equal numbers. Thus, in the cone axon there appear to be two overlapping sets of actin filaments whose opposite polarities correspond to the two actin halves of a muscle sarcomere.

In elongated, dark-adapted cones, thick filaments are localized throughout the axon region of the cone. In light, thick filaments accumulate toward the proximal end of the cone.

These observations are consistent with a "sliding hypothesis" for cone contraction, in which thick myosinlike filaments produce sliding interdigitation of the two sets of oppositely directed actin filaments in the proximal axon region. Thus, the myoid thin filaments would be essentially reeled into the axon region to produce shortening. The mechanism of re-elongation depends on microtubules, as discussed in the companion paper.

Our understanding of the structural basis for contraction in nonmuscle cells is still at a primitive stage. Although we may now assume with some certainty that actin and myosin are present in all eukaryotic cells, and though we have characterized many properties of the cytoplasmic myosins, actins, and actin-associated proteins, we nevertheless know little about how the cell deploys its actin and myosin to bring about contraction (15). We do not even know whether actin and myosin interact in filamentous forms analogous to those in muscle; in fact, other alternatives have been suggested (30, 33). Our persisting ignorance derives in part from the complexity of the contractile phenomena in nonmuscle cells and in part from unresolved difficulties in preserving and discerning both actin and myosin filaments in electron microscope studies of these cells (30).

To minimize the problems of complexity, I have looked for a cell in which contraction is linear, slow, and repetitive. Linearity of contraction permits quantitation, while slowness permits investigation of intermediate stages. In a repetitive contractile phenomenon, there is greater probability that the contractile apparatus will be a constant structural feature, so that the mechanism of contraction may be dissociated from the problem of dis- and reassembly of the contractile apparatus (30, 33). The teleost retinal cone (9) possesses these advantages and thus provides a promising model for a structural study of nonmuscle contraction.

The long, slender cones of many fishes shorten in response to light (Fig. 1). Shortening does not take place equally over the entire length of the cell, but rather is restricted almost exclusively to a central necklike region called the myoid. This myoid undergoes extreme shortening (from 85 μm to 5 μm in length in some species) at a relatively slow rate (1-3 μm/min; references 2, 9). Thus, cone shortening is slow and linear. Shortening is also repetitive; cones daily shorten in the light and elongate in the dark. These cone movements, along with closely integrated movements of rods and retinal pigment, serve to adapt the fish eye to day or night vision (2, 34). In the day, cones shorten to move their outer segments toward the bright incoming light while rods elongate to bury their outer segments in the shielding

retinal pigment. At night, these movements are reversed so that the rod outer segments are first in line for reception of any faint, incoming light.

Two observations suggest that cone shortening is an active contractile process. First, disruption of the many microtubules present in the myoids of dark-adapted cones by colchicine, high pressure, or low temperature does not produce myoid shortening in the absence of light (9, 35). Thus, it seems unlikely that shortening results from the collapse of the microtubule cytoskeletal system present in the elongate myoid. Second, light-induced cone shortening is blocked by cytochalasin B (9). Though the precise mechanism of action of cytochalasin B has not been elucidated (16, 38), this drug has been found to block actin-associated contractile phenomena in many cell types (8, 12, 22, 31, 39). Blockade of cone contraction with cytochalasin therefore suggests that cone shortening is an active contractile process comparable to previously studied examples of nonmuscle contraction.

A previous paper has described longitudinally oriented thin and thick filaments in teleost cones and also demonstrated that the thin filaments in teleost cones are actin by myosin subfragment-1 (S-1) binding (9). In this paper, those observations are extended to consider the distribution of actin filaments in light- and dark-adapted cones, as well as the polarity of the actin filaments. Finally, possible implications of these observations for the mechanism of cone contraction are discussed. The role of myoid microtubules in the complementary dark-induced elongation of the teleost cone is considered in a companion paper (35).

MATERIALS AND METHODS

Animals

Three species of fish were used for these studies according to their availability in Bermuda, Philadelphia, or Berkeley. Most of the studies use the Bermudian blue stripe grunts (*Haemulon sciurus*) and grey snappers (*Lutjanus griseus*). Acquisition and maintenance procedures for these fish have been described in a previous paper (9). For experiments in Bermuda, both snappers and grunts were used to assure a continual supply of research animals as neither species could be collected with certainty at all times. Myosin S-1 binding experiments were performed on eyes from grunts and from killifish (*Fundulus heteroclitis*) obtained from bait stores near Philadelphia and maintained in salt-water aquaria at 70°F in the lab. Because grunts and snappers did not survive shipment to Philadelphia, the locally available

killifish was used for myosin S-1 experiments at the Philadelphia laboratory. Probably because fresher myosin S-1 could be used in these cases, better decoration was obtained in the *Fundulus* experiments, and these have been used for the polarity studies. Similar decoration results were obtained in grunt retinas, but arrowheads were not so clearly discernible. Except for the greater extent of cone elongation in grunts, the light-induced shape changes, the fixation quality, and the distributions of thin and thick filaments in cones were not detectably different in the three species studied.

Dark-adapted fish were dissected and handled in dim red light from a Wratten 1 filter. This light did not induce cone contraction. Fish were maintained on an artificial light-dark cycle (14 h light: 10 h dark) and used for light- or dark-adapted states at appropriate times in the cycle.

Procedures for fixation and embedding of squirrel monkey and rat retinas have been described in an earlier paper (10, 11).

Electron Microscopy

Immersion fixation, embedding, sectioning, and staining procedures for electron microscopy have been previously described (9). New procedures introduced in this paper are perfusion fixation, a special *en bloc* staining procedure which stains thick filaments very intensely, and direct OsO₄ fixation without aldehydes.

Perfusion fixation was carried out according to the method of Copeland (14) using several fixatives. Best preservation of actin filaments was obtained with 2% glutaraldehyde (Fisher or Polysciences biological grade) in 0.1 M phosphate or 0.1 M cacodylate, pH 7.0; fixatives containing paraformaldehyde or EM grade glutaraldehyde did not preserve actin filaments so well. Retinas were perfused *in situ* for 30 min, dissected to expose the posterior eyecups which were transferred to fresh fixative, and left for 1 h at room temperature. Retinas were then cut into squares and left in cold fixative overnight. Postfixation was carried out in 1% OsO₄ for 30 min to 1 h in the cold. Some retinas were *en bloc* stained with 0.5% aqueous uranyl acetate for 1 h in the dark. Dehydration and embedding procedures were those described by Burnside (9).

Some retinas were fixed in 2% OsO₄ in Standard Salt Solution (0.1 M KCl, 2 mM MgCl₂, 10 mM phosphate buffer, pH 7.0), *en bloc* stained in aqueous uranyl acetate (0.5%) for 1 h, and then dehydrated and embedded as usual (9).

Dense staining of thick filaments was obtained in retinas which were treated as follows: Retinas were perfused with 2% glutaraldehyde, 1% paraformaldehyde in Standard Salt Solution (0.1 M KCl, 2 mM MgCl₂, 10 mM phosphate buffer, pH 7.0), postfixed as described above, left in aqueous 0.5% uranyl acetate in the dark at room temperature for 8 h and in the cold for 10 more h, and then dehydrated and embedded as usual. This procedure has not given consistent dark staining of

thick filaments on all repetitions, but both light-adapted and dark-adapted eyes with heavily stained filaments have been obtained.

Preparation and Negative Staining of Isolated Cones

Procedures for retinal dissociation, enrichment for isolated cones, and negative staining of detergent-disrupted cones have been described in a previous paper (9).

Myosin Subfragment-1 Binding

Myosin S-1 binding studies were performed on retinas from killifish and from blue striped grunts according to procedures described in a previous paper (11).

Determinations of Arrowhead Polarity on Actin Filaments in Cone Axons

From myosin S-1-treated, light-adapted *Fundulus* retinas, three different regions of the cone axon were photographed for study: (*a*) near the outer limiting membrane, (*b*) mid axon, and (*c*) near the synaptic pedicle. Low-magnification shots for orientation and high-magnification shots for polarity determination were taken. Duplicate prints (not identified as to location) were marked by three observers to indicate polarities of discernible arrowheads. Numbers of proximally and distally directed arrowheads as well as all discernible arrowheads with other orientations were tabulated, and percents of arrowheads directed proximally and distally were calculated for each micrograph. All percents for each micrograph were then averaged, and the standard error was calculated for each of the three regions.

Because in the distal myoid and ellipsoid part of the cone the arrowheads were almost exclusively proximally directed, no quantification of this region was carried out.

RESULTS

Morphology of the Cone Cell

Fig. 1 contrasts the morphologies of light- and dark-adapted cones from the grey snapper, *Lutjanus griseus*. Similar shape changes between light- and dark-adapted states are observed in cones of most bony fish which are adapted to both day and night feeding (3).

Some parts of the cone are free to move, and others are not. At the outer limiting membrane (see Fig. 1), cones are attached to the retinal supportive cells (Müller cells) by adherens junctions. The part of the cone above the outer limiting membrane is free to move within the compartment between the neural retina and the pigmented retinal epithelium. The part of the
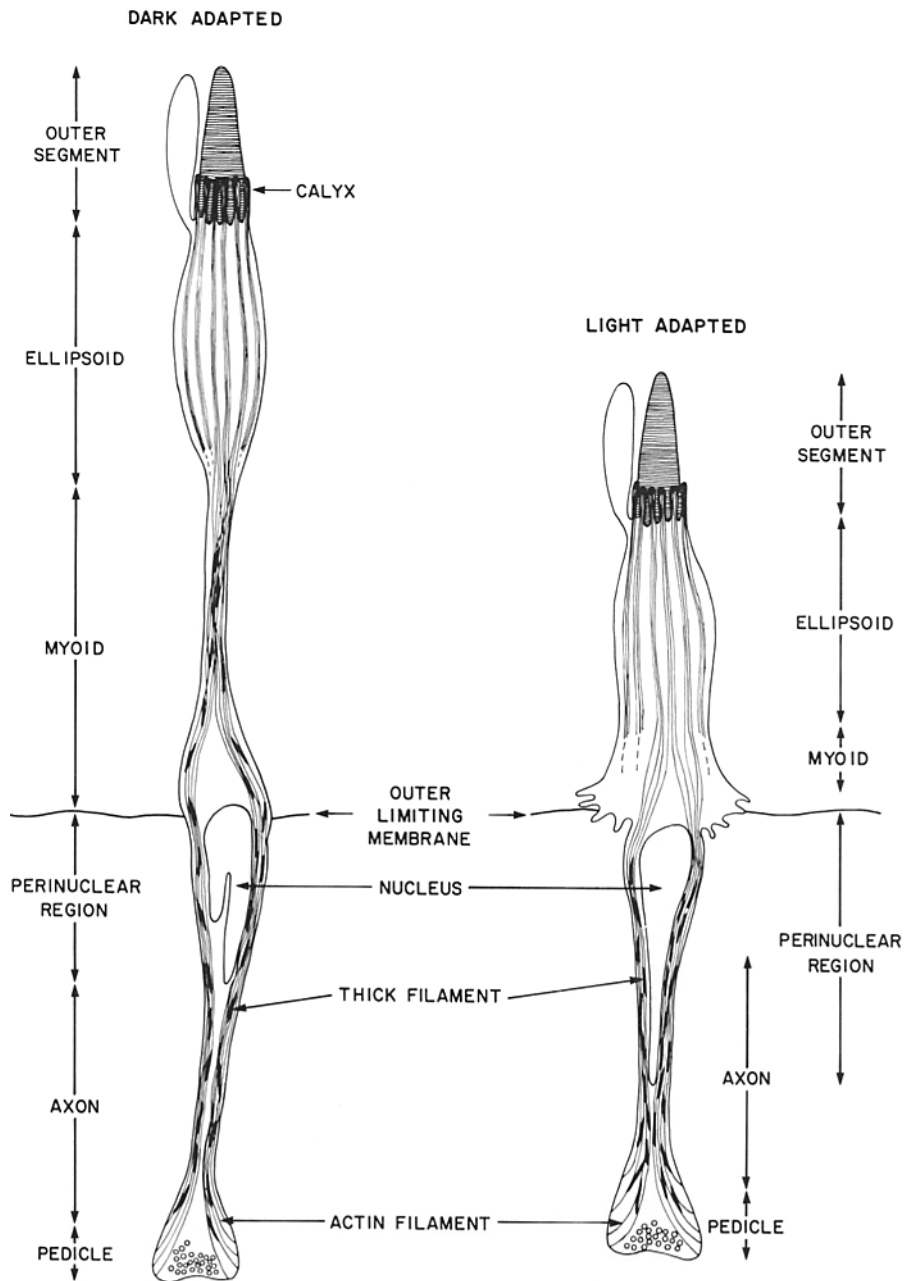
FIGURE 1 Schematic illustrations of differences in morphology and of distributions of thin and thick filaments between dark-adapted and light-adapted cones.

cone below the outer limiting membrane, on the other hand, is relatively fixed. This proximal part of the cone is closely associated with rod nuclei and axons and with Müller cell projections.

Essentially all of the cone's light-induced contraction takes place in the myoid (see Fig. 1). In the dark-adapted snapper, the narrow necklike myoid is extended to approx. 30 μm in length. In the light, this myoid becomes broader and shorter until the ellipsoid lies only a few micrometers above the nucleus. As a result of the large decrease in myoid surface area which accompanies
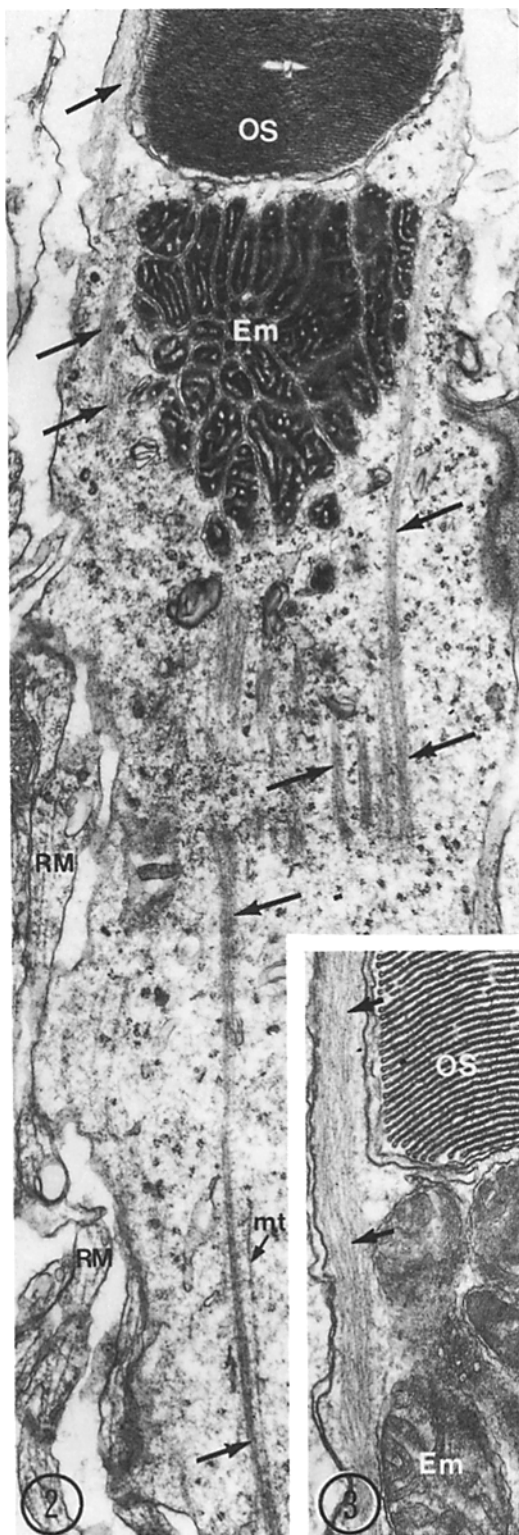
shortening, the myoid plasma membrane is thrown into elaborate longitudinal flutes and folds which project between adjacent photoreceptors.

The morphology and location of the nucleus differ in light- and dark-adapted cones (Fig. 1). In the light-adapted cone, the nucleus sits well below the outer limiting membrane and is elongated proximally into a tapered process which extends deep into the axon. In the dark-adapted cone, the nucleus lies closer to the OLM and is less elongated, and contains deep indentations which extend from the proximal toward the distal surface of the nucleus (Fig. 1).
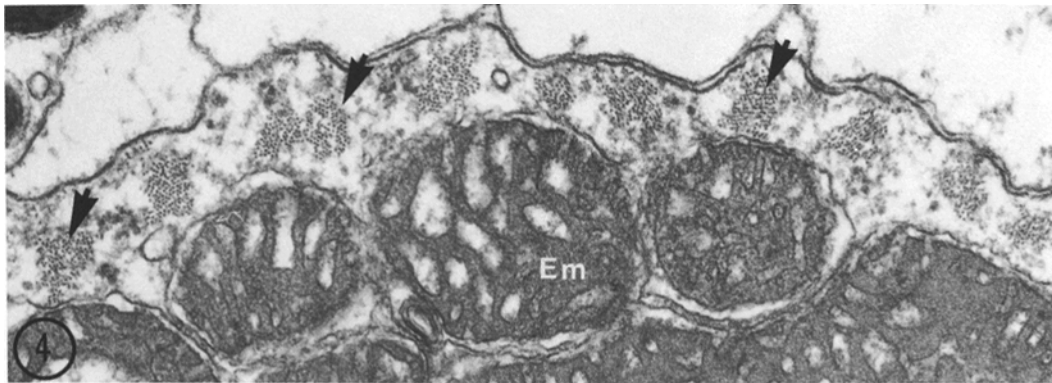
Thin Filaments

The distributions of thin filaments in light- and dark-adapted cones of the grey snapper are illustrated schematically in Fig. 1. Although some aspects of the distribution of thin filaments shown in Fig. 1 have been previously described (9), this paper incorporates new information, especially in the myoid, perinuclear, and axon regions, which has been obtained from recent fixation improvements and myosin S-1 decoration studies. For clarity, the entire distribution is summarized here.

Ellipsoidal Filaments

The longitudinally oriented bundles of thin filaments shown in Fig. 1 begin as core filaments of microvilluslike projections (calyces) which embrace the proximal end of the cone outer segment (Figs. 1–3). At this level, the bundles are similar in size and packing arrangement to the core filaments of intestinal microvilli (32), and, like those filaments, originate in dense tips at the distal

FIGURE 2 Ellipsoid thin filaments: longitudinal section passes through outer segments (OS), ellipsoid mitochondria (Em), and peripheral ellipsoid cytoplasm. The outer limiting membrane and short myoid lie just below the bottom of the figure. Bundles of thin filaments (arrows) extend the full length of the ellipsoid; because this section is slightly tangential, bundles pass into and out of the plane of the section. mt, microtubules; and RM, rod myoids. (Light-adapted grey snapper: OsO₄ fixation). × 19,600.

FIGURE 3 Ellipsoid thin filaments: longitudinal section through microvillus-like projection (calyx) at base of outer segment (OS). The filament bundle of the process (arrows) continues into the peripheral cytoplasm of the ellipsoid between the plasmalemma and the central mitochondrial mass (Em). (Light-adapted grey snapper: perfusion fixation. × 39,000.

FIGURE 4 Ellipsoid thin filaments: transverse section through the ellipsoid region showing thin filament bundles (arrows) in peripheral cytoplasm. *Em*, ellipsoid mitochondria. (Light-adapted killifish: immersion glutaraldehyde fixation. × 54,000.

end of the projection (not shown). The cone filament bundles do not terminate at the base of the microvilluslike projections but rather continue for the full length of the ellipsoid (Fig. 1). These bundles (18–22/cell) lie in the peripheral cytoplasm between the large central mass of ellipsoid mitochondria and the plasmalemma (Figs. 2 and 4). Light- and dark-adaptive cone movements produce no significant changes in the distribution or packing of the ellipsoid filament bundles.

Several observations suggest that the thin filaments of the ellipsoidal bundles are cross-linked to one another. The filaments in the bundles maintain a relatively regular filament-to-filament spacing (measurements average 10.6 ± 2.0 nm; n = 50), and stray filaments are rarely seen around the periphery of the bundle (Fig. 4). Also, the ellipsoidal filament bundles remain intact during disruption of isolated cones with detergent for negative staining (Fig. 5). Myosin S-1 decoration of ellipsoidal thin filaments in glycerinated cones

occurs only if the ellipsoidal bundles are disrupted (splayed), though thin filaments in other parts of the same cone do bind S-1 to form arrowheads. The observation that intact ellipsoidal bundles (with typical filament-to-filament spacing) do not decorate suggests that S-1 is excluded by the tight packing or that cross-linkers occupy or obstruct the S-1 binding site. In either event, this observation suggests that the thin filaments are held together. Finally, the actin filaments of the ellipsoidal bundles are considerably more stable to conventional fixation than the actin filaments in the rest of the cone; they are present in almost all fixed preparations while myoid filaments (see below) are frequently not preserved.
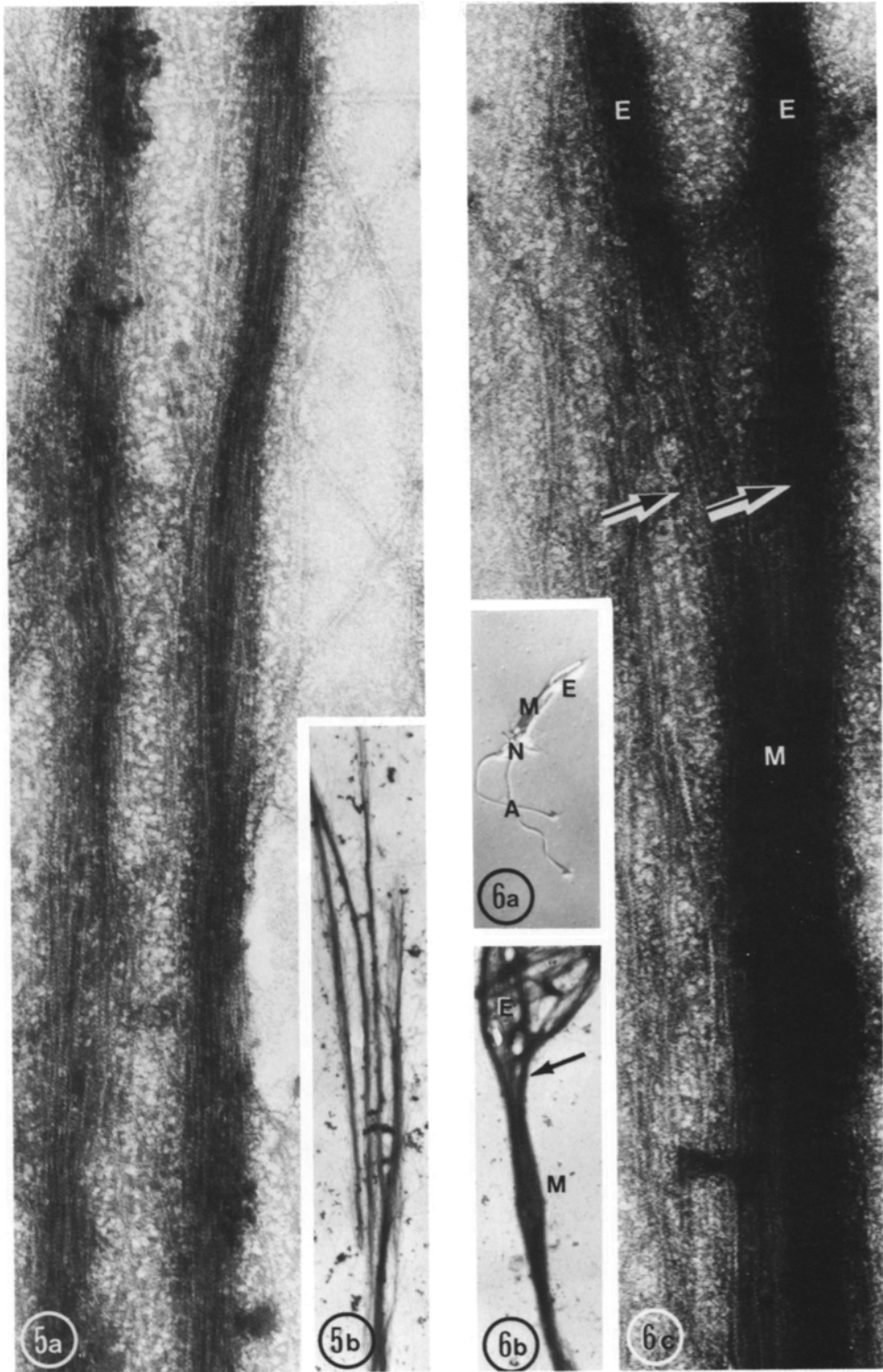
Myoid Filaments

Filaments of the ellipsoid bundles continue into the myoid region of the cone (Figs. 1 and 6). In both light- and dark-adapted cones, the ellipsoid bundles splay into more loosely aggregated arrays

FIGURE 5 Ellipsoid filament bundles from isolated, dark-adapted grey snapper cone (see Fig. 6 *a*), disrupted with 1% Triton X-100 and negatively stained with uranyl acetate. (*a*) At high magnification, the beaded substructure of actin filaments is visible. × 135,000. (*b*) Though some bundles splay into individual filaments, most remain intact. The bundles are usually straight as though stiff. Bundle diameter approximates that seen in section in Fig. 4. × 7,500.

FIGURE 6 Myoid and ellipsoid thin filaments from a dark-adapted, isolated twin cone from grey snapper disrupted with Triton X-100 and negatively stained with uranyl acetate. (*a*) Nomarski light micrograph illustrating the ellipsoid (*E*), myoid (*M*), nuclear (*N*), and axon (*A*) regions of the isolated cone; because this example is a twin cone, all the indicated parts are paired. × 500. (*b*) Myoid (*M*) and ellipsoid (*E*) thin filaments remain on the grid after detergent disruption of the cone. The bundles in the ellipsoid region are continuous with the looser skein of thin filaments in the myoid region (arrows). × 8,000. This continuity is shown at higher magnification in (Fig. 6*c*) (arrows). (Grey snapper). × 143,500.

of longitudinally oriented filaments as they enter the myoid.

In the long myoid of the dark-adapted cone, the loose skein of filaments usually comprises a more or less continuous sheath of thin filaments just beneath the myoid plasmalemma (Figs. 1, 7). This sheath of myoid filaments may also be seen in negatively stained preparations of detergent-disrupted, dark-adapted cones (Fig. 6). That ellipsoidal filaments are continuous with myoid filaments is clearly demonstrated in negatively stained preparations where the stalk of myoid filaments may be seen to split into bundles with diameters appropriate for ellipsoidal bundles (Fig. 6; also see Figs. 7 and 9 in reference 9).

In light-adapted cones, the myoid is only a few micrometers in length (Fig. 1). Thus, the ellipsoid-myoid junction (where the ellipsoid bundles splay into looser skeins of filaments) lies much closer to the nucleus than in dark-adapted cones. Thin filaments traverse this broad short myoid region in loosely associated groups (Fig. 8). The plasmalemma in the myoid region assumes elaborate longitudinal flutes and folds (Fig. 8b). The myoid filaments are not associated with the entire circumference of the plasmalemma, as they are in dark-adapted cones, but instead tend to occupy a more central location, being generally absent from the flutes (Fig. 8b).

The thin filaments of the cone's myoid are extraordinarily labile to fixation and embedding procedures. In contrast to the findings of Pollard et al. (reference 30; using actin filaments in vitro), the cone thin filaments are well preserved in fixations with OsO₄ alone without glutaraldehyde fixation, though overall fixation of the retina is distinctly inferior in these cases (see Fig. 2). The distributions of myoid thin filaments reported here have been observed in six different retinas (fixed by both OsO₄ and conventional glutaraldehyde procedures) and have been corroborated with glycerinated, S-1 decorated preparations where thin filaments are clearly observed. Nonetheless, more than 50 retinas were examined in which myoid thin filaments were not clearly discernible.

Perinuclear and Axonal Filaments

Loosely associated groups of longitudinal filaments are present in the perinuclear region. The number of these filament groups (<10) is significantly less than the number of ellipsoid filament bundles. Bundles of filaments with regular packing typical of the ellipsoidal filaments are not found in axon or perinuclear regions. Because the filaments are not arranged in closely packed bundles and because the cytoplasm is usually more dense in these regions, it has been difficult to ascertain the distribution of filaments here. Even in retinas where some cones show clearly the distribution described in Fig. 1, other cones seem devoid of recognizable thin filaments. Numerous thin filaments are seen, however, in glycerinated preparations (Fig. 9d). From these, it is clear that numerous axially oriented filaments occupy most of the space in the cone axon. Microtubules are also present in this axon region. It has not been possible to ascertain whether different numbers of filaments are found in the axon region in light- as opposed to dark-adapted cones, because of the difficulties of fixation and clear visualization described above and because of the disordering of overall structure produced by glycerination (Fig. 9d-e).

Polarity of Thin Filaments

The polarity of the cone's longitudinal actin filaments has been ascertained by examining cones whose thin filaments have been decorated by incubation with myosin S-1 (Fig. 9). In ellipsoids and myoids of dark-adapted cones, the arrowheads on almost all filaments are proximally directed, i.e., they point away from the tips of the calyces toward the synaptic pedicle (Fig. 9a, b). Thus, for ellipsoid and myoid filaments, the distal tip of the microvillus corresponds to the Z-line attachment of actin filaments in the skeletal muscle sarcomere. In the more proximal part of the myoid, occasional filaments have arrowheads pointing in the opposite direction (distally directed; Fig. 9c). Polarities of filaments in axons of dark-adapted cones have not been discernible because of the disruption of the outer nuclear layer by glycerination in dark-adapted retinas; cone axons are not recognizable though many decorated filaments are about.

Decorated filaments are more clearly preserved in light-adapted cones (Fig. 9d-j). All ellipsoidal filaments and those of the short myoid region are proximally directed as they were in the dark-adapted cone. In the axonal region of the light-adapted cone, two groups of filaments are found: filaments bearing proximally directed and those bearing distally directed arrowheads (Fig. 9d-i and Table I). More than 90% of observed filaments are axially oriented. The percent of distally directed arrowheads increases as one proceeds
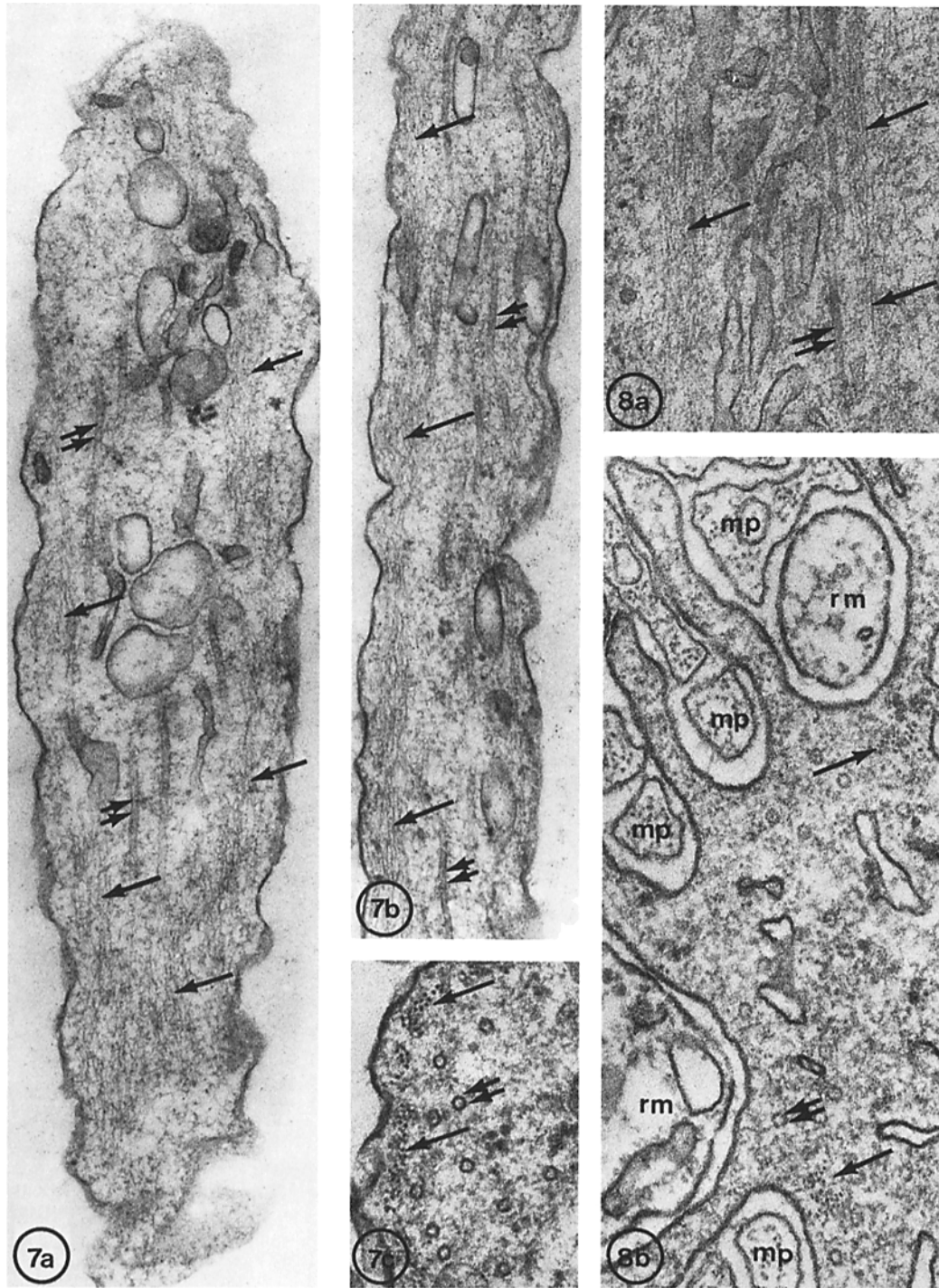
FIGURE 7 Myoid thin filaments in a dark-adapted cone: tangential (a), longitudinal (b), and transverse (c) sections through the elongate myoid region. Note that peripheral thin filaments (single arrows) are not grouped into bundles like those in ellipsoid. Microtubules (double arrows) are present in the central part of the myoid. (Blue-striped grunt: immersion glutaraldehyde fixation) (a and b) × 62,000; (c) × 84,000.

FIGURE 8 Myoid thin filaments in a light-adapted cone: longitudinal (a) and transverse (b) sections through the myoid region. This region contains longitudinally oriented thin filaments (single arrows) and microtubules (double arrows). These filaments are more loosely grouped than the filaments of the ellipsoid bundles in Fig. 4. The plasma membrane of the myoid region in light-adapted cones is thrown into axial flutes which project between the nearby rod myoids (rm) and apical projections of Müller cells (mp). (Blue-striped grunt: immersion glutaraldehyde fixation). (a) × 62,000; (b) × 83,000.

from the nucleus toward the synaptic pedicle, until near the pedicle the numbers of proximally and distally directed arrowheads are approximately equal (Table I and Fig. 9 f–i). Decorated filaments are also present in the cone pedicles but, because of the swollen state of the pedicles after glycerination, oriented filaments are rarely observed. In rare cases, where oriented filaments and arrowheads are visible, the arrowheads appear to be mostly distally directed (Fig. 9j). However, the disruption of pedicle morphology makes it impossible to discern the origins of those axon filaments with distally directed arrowheads.

Thick Filaments

Thick filaments, averaging 14 (±1.6) nm in diameter, are found in the myoid, perinuclear, and axonal regions of the teleost cone (Figs. 1 and 10). These filaments possess periodic lateral sidearms with a repeat of approx. 15 nm (15.4 ± 1.5 nm, Fig. 10b; see also reference 9). The distributions of thick filaments in light- and dark-adapted cones have been compared in preparations in which thick filaments are preferentially stained intensely with uranyl acetate (Fig. 10c; see Materials and Methods). The very dense stain made it possible to recognize even single thick filaments in cross and longitudinal section though thin filaments were not well preserved.

The distributions of thick filaments in light- and dark-adapted cones ascertained from these studies are illustrated in Fig. 1. The long myoid of the dark-adapted cone contains scattered single thick filaments usually, but not always, oriented longitudinally (Fig. 10d). Most of the thick filaments, in both light- and dark-adapted cones, are found in the perinuclear and axonal regions (Fig. 10a–c, e–g). These thick filaments are longitudinally oriented and often collected near the mid-axon into a single large group (Fig. 10a, b) which branches at either end into smaller groups (Fig. 10e–g). These smaller branches extend into the pedicle at the proximal end and embrace the nucleus at the distal end (Fig. 10e and g). The only noticeable light-dark difference in filament distribution in the perinuclear and axonal region is an apparent accumulation of thick filaments toward the proximal (synaptic) end of the cell in the light-adapted state.

In cross sections of axon thick filaments, the filaments were often found to be aggregated laterally into anastomosing ribbonlike structures

(Fig. 10a, c). The degree of lateral association varied in different preparations. In preparations adjudged to be best fixed by other criteria, the thick filaments were least aggregated (see also reference 9).

Cone thick filaments clearly differed from 10-nm neurofilaments of adjacent nerve fibers of the outer plexiform layer, with respect to size, tendency to aggregate laterally, and staining reaction in the densely stained preparations (Fig. 11a, b).

DISCUSSION

Light-induced cone contraction has been examined in an attempt to elucidate the structural basis for nonmuscle cell contractility. Cone cells possess longitudinally oriented actin filaments of two polarities: filaments with proximally directed arrowheads are found at all levels of the contracted cone, and filaments with distally directed arrowheads are found in the axon. The distributions of these filaments suggest that they are disposed into two overlapping groups having opposite polarity. The polarities of the two groups of filaments correspond to those of the two actin halves of the skeletal muscle sarcomere. Cone cells also possess longitudinally oriented thick filaments, having appropriate diameter and sidearm spacing to be myosin filaments. These thick filaments are localized in the same part of the cone where the two oppositely directed sets of actin filaments overlap (the axon), and they appear to accumulate toward the proximal end of the cone during contraction. Before we examine the implications of these observations regarding possible models for the mechanism of cone contraction, it is first cogent to evaluate the evidence that the thin and thick filaments described are in fact actin and myosin filaments.

Thin Filaments

That the cone thin filaments are in fact actin is well established. Negatively stained cone thin filaments exhibit the beaded substructure typical of muscle actin, and the filaments bind myosin S-1 to form arrowheads typical for skeletal muscle actin (17, see also reference 9).

Thick Filaments

Because clear-cut diagnostic procedures such as those for actin filaments are not yet available for myosin filaments in nonmuscle cells, the evi-

Table I

Distributions of Actin Filaments with Proximally and Distally Directed Arrowheads in Specified Regions of S-1 Decorated, Light-Adapted Fundulus Cones

	Proximally directed arrowheads	Distally directed arrowheads	Total number arrowheads counted	Number micrographs examined
	% ± SE	% ± SE		
Near outer limiting membrane	89 ± 3	5 ± 2	822	7
Mid-axon	69 ± 6	21 ± 5	522	7
Near pedicle (synapse)	46 ± 9	47 ± 10	555	7

Arrowheads on filaments not oriented parallel to the axis of the cone were included in totals; these arrowheads were less than 10% in all three regions. See Materials and Methods for explanation of procedures.

dence that cone thick filaments are myosin is more circumstantial than that for actin. Nevertheless, several observations favor this conclusion. Though smaller than myosin filaments of skeletal muscle, cone thick filaments have dimensions and morphology similar to those of filaments formed in vitro from several nonmuscle myosins (1, 30) and to thick filaments observed in thin sections of other nonmuscle cells, such as amoebae (6, 25, 28), blood platelets (5, 40), slime molds (20), and intestinal epithelial cells (24). Cone thick filaments have sidearms with a periodicity (~15 nm, reference 9) that closely corresponds to that of skeletal muscle myosin (17). Cone thick filaments clearly differ, both in size and in staining reaction (see Figs. 10 and 11), from 10-nm neurofilaments in the neuronal processes of the nearby outer plexiform layer of the retina.

Cone thick filaments tend to aggregate laterally into ribbonlike structures reminiscent of those produced by myosin filaments in smooth muscle after immersion fixation (21). This aggregation of smooth muscle thick filaments appears to result as an artifact of slow immersion fixation as no aggregation occurs during perfusion fixation or freeze substitution (7). Some aggregation of thick filaments is observed in teleost cones even after perfusion fixation, presumably because penetration of fixative into the avascular teleost retina is slower than that obtained in more highly vascularized smooth muscle.

The species distribution of cone thick filaments

Figure 9 Myosin S-1 decoration of actin filaments in light- and dark-adapted cones of Fundulus. (a) Long dark-adapted (DA) cone with decorated ellipsoid (E) and myoid (M) filaments. OS, Outer segments; black square indicates region shown in Fig. 9b. × 21,000. (b) Higher magnification of myoid region indicated by the square in Fig. 9a. Arrowheads are predominantly directed toward the proximal end of cone (arrows). × 100,000. (c) Lower myoid near the nucleus of DA cone. Occasional distally directed arrowheads (double arrows) are found. Single arrows indicate proximally directed arrowheads. × 105,000. (d) Axon region proximal to nucleus in a light-adapted cone in which glycerination failed to produce usual swelling and extraction. The axon contains numerous thin filaments (arrows) not decorated with S-1. N, nucleus. × 34,000. (e) Axon region, equivalent to that in Fig. 9d, of an LA cone which exhibited typical swelling and extraction after glycerination. The axon filaments (arrows) in this cell are decorated. N, nucleus. × 34,000. (f) Survey of S-1 decorated LA cone cell. Ellipsoid (E) mitochondria and extracted nucleus (N) permit identification of cone axon (A) with its numerous SER vesicles and decorated filaments. × 7,250. (g) Decorated filaments from mid-axon region of LA cone. Both proximally directed (single arrows) and distally directed arrowheads are present. × 90,000. (h) Decorated filaments from perinuclear region near outer limiting membrane. Most filaments have proximally directed arrowheads (single arrow), but some distally directed arrowheads are present (double arrows). × 44,000. (i) Decorated filaments in the proximal region of an axon (near synapse) from an LA cone. The proportion of distally directed arrowheads (double arrows) is greatest in this region of the axon (see Table I). Single arrows, proximally directed arrowheads. × 44,000. (j) Pedicle (synapse) region of LA cone. Some decorated filaments can be discerned. Though determination of polarity is more difficult here, most arrowheads appear to be distally directed (double arrows) × 44,000.
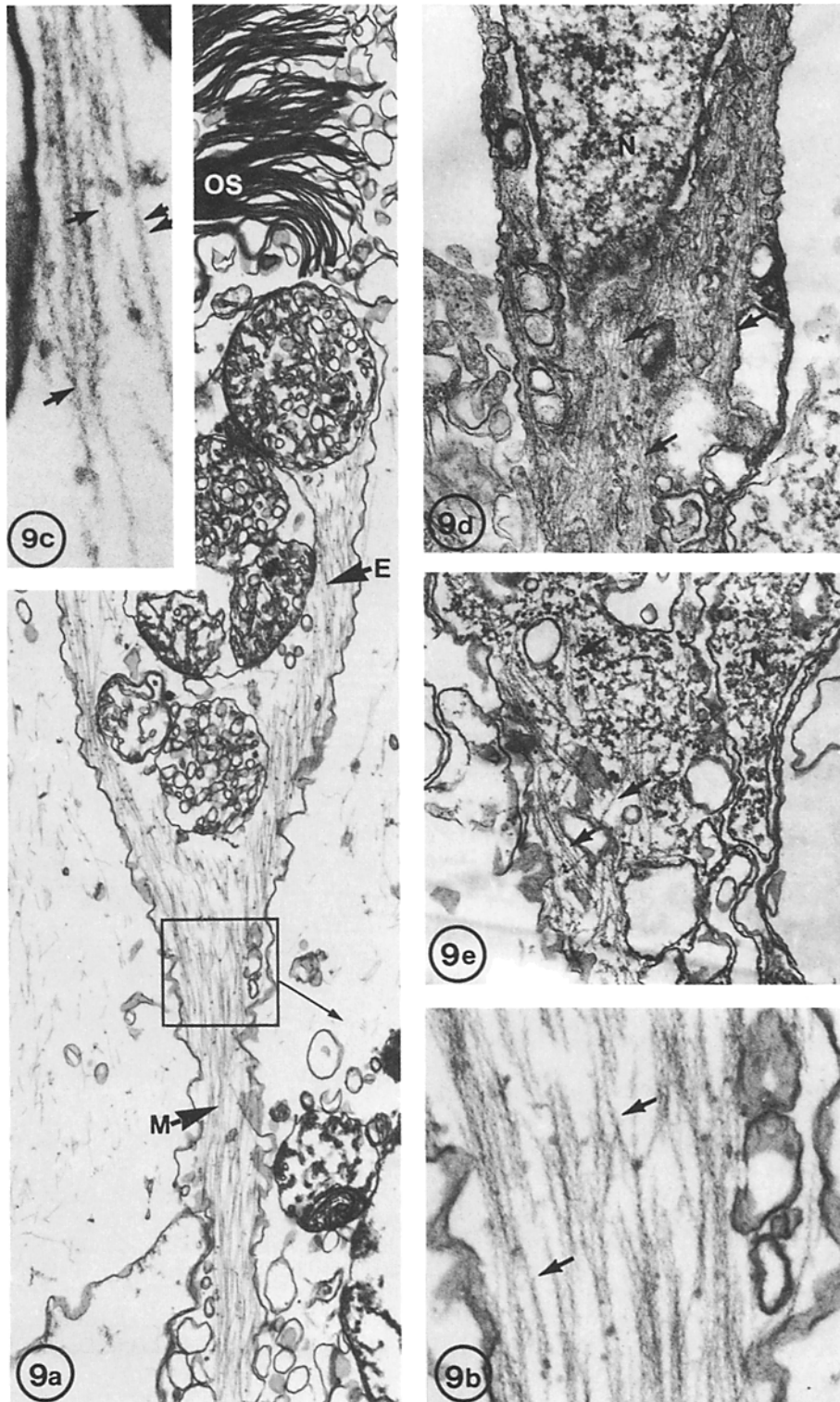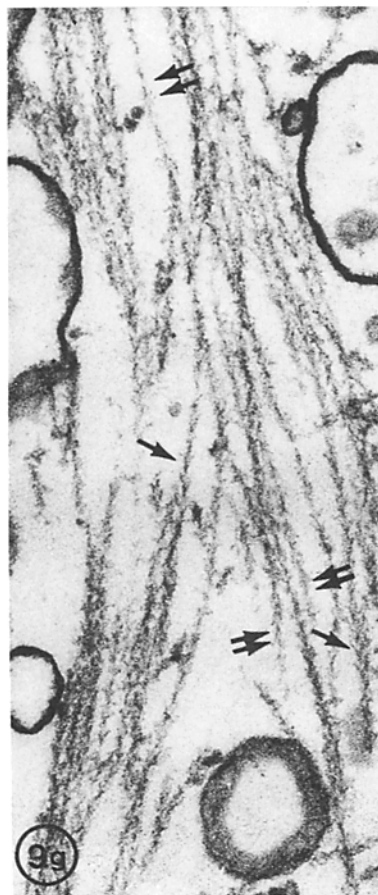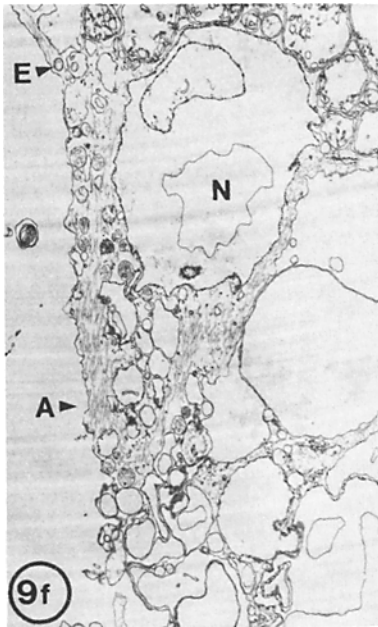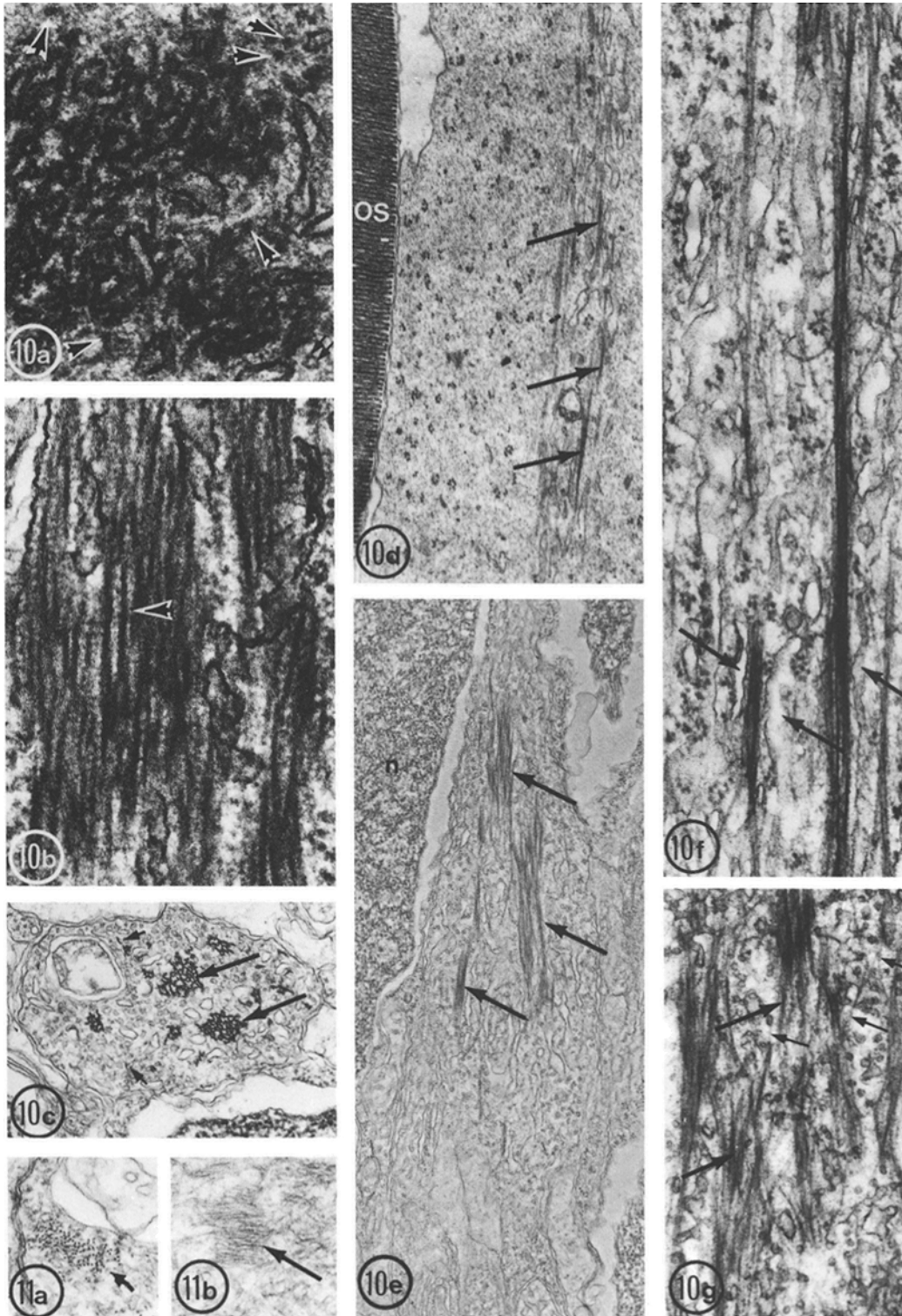
correlates with the presence of photomechanical contraction. Thick filaments are absent from the noncontractile cones of mammals (2).

Studies are now in progress to ascertain whether fluorescent antibodies to fish brain myosin will localize in those parts of the cone where thick filaments are observed. Until now, no other examples of cytoplasmic thick filaments have been clearly documented to be myosin by antibody staining, primarily because it has not been possible to correlate the specific localization of thick filaments in sections and the antibody labeling in the same cell type (26, 27, 30, 37). The specific localization of thick filaments inthe long cone cells should make such a study possible.

It should be pointed out here that the presence of thick filaments in the cone axon in fixed preparations does not prove unequivocally that myosin exists in the filamentous state in vivo, especially because the preservation of thick filaments is so variable. Nonetheless, this localization of thick filaments in the axon almost certainly reflects the distribution of myosin in the cell, and it is this distribution that is functionally significant in the discussion of mechanism which follows.

Structural Basis for Teleost Cone Contraction: a Sliding Hypothesis

The distributions of thin and thick filaments and the polarities of thin filaments reported here clearly suggest a model for cone contraction based on the sliding hypothesis for skeletal muscle (18, 19). A hypothetical sliding model for cone contraction is illustrated in Fig. 12. According to this model, the cone's overlapping distal (myoid) and proximal (axon) sets of thin filaments correspond in polarity to the two halves of a single skeletal muscle sarcomere, i.e. the ends of the cone cell would correspond to the sarcomere Z-line attachments, with arrowheads pointing away from the Z-lines (17). This model differs from the muscle sarcomere in that the filaments of the two "half-sarcomeres" overlap, slightly in the dark-adapted cone, and completely in the light-adapted cone. Bipolar thick filaments would be present in the region of overlap in both long and short cones.

According to the model, when the cones are exposed to light, sliding would be initiated by those myosin filaments whose bridges contact actin filaments of opposite polarity. Myosin bridge activity would then tend to exert a pull on the two half sarcomeres, increasing their overlap, and consequently shortening in the cell. Because the proximal (axonal) half of the cell is fixed to its cellular neighbors, shortening would be accommodated totally by the myoid half which is free to move. Thus, myosin filament bridge action would tend to reel in myoid thin filaments and at the


FIGURE 10 Thick filaments from cones: (a) Transverse section of central group of thick filaments at mid-axon level. Some individual filaments are visible (arrows) though most filaments appear to have aggregated laterally; thick filaments are 14 nm in diameter (compared to microtubule, double arrows) (light-adapted grey snapper: glutaraldehyde perfusion fixation). × 83,000. (b) Longitudinal section of cone thick filaments at mid-axon from same retina shown in Fig. 10a. Note the periodic sidearms (arrows). These have a repeat of approx. 15 nm. × 90,000. (c) Transverse section of cone axon in snapper retina prepared by special techniques which intensely stain thick filaments. This section is closer to the pedicle (synaptic ending) and many synaptic vesicles are present. The dense stain makes even small groups of filaments visible (small arrow) (dark-adapted grey snapper-mixed aldehyde perfusion fixation). × 26,000. (d) Myoid of dark-adapted cone. Thick filaments are scattered and relatively rare. OS, outer segment of nearby rod. (Dark-adapted grunt:glutaraldehyde immersion fixation). × 19,000. (e) Perinuclear region of cone axon. Thick filaments are present in small groups (dark-adapted grey snapper:perfusion glutaraldehyde fixation). × 38,000. (f) Proximal axon region of DA grey snapper cone. Smooth ER is abundant in the cone axon. Cisternae are often seen near thick filament bundles (arrows). × 62,000. (g) Proximal region of cone axon near synapse. Thick filaments are present in small groups. Small arrows indicate possible thin filaments interdigitating with thick filaments. (Light-adapted grey snapper: glutaraldehyde immersion fixation) × 56,000.

FIGURE 11 10-nm neurofilaments (arrows) in nearby outer plexiform layer of the same retina illustrated in Fig. 10c. In cross (Fig. 11a) and tangential (Fig. 11b) sections, these filaments clearly differ both in size and in staining characteristics from the thick filaments of the cone axon. (Dark-adapted grey snapper. × 35,000.
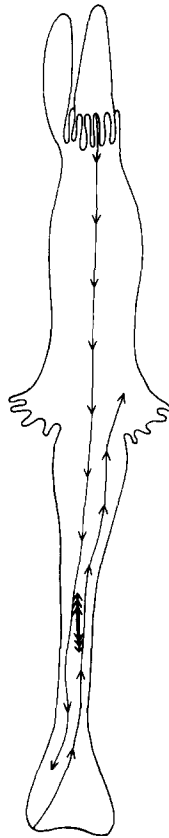
DARK ADAPTED
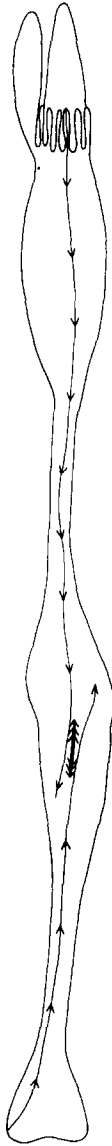
LIGHT ADAPTED

FIGURE 12 Hypothetical model for the mechanism of teleost cone contraction based on the sliding filament hypothesis from skeletal muscle. Groups of thin filaments of opposite polarity overlap in the midregion of the cone. Thick filaments are found in the region of overlap. Because the proximal (axonal) half of the cone is fixed to its cellular neighbors, only the distal half is free to shorten. Thus, initiation of sliding by thick filaments would result in further interdigitation of the two sets of thin filaments in the proximal axon region, accumulation of thick filaments toward the proximal end of the cell, and shortening of the myoid region.

same time tend to displace the myosin filament along the fixed axonal filaments toward the synaptic end of the cell. With increased overlap, the myoid half sarcomere would be pulled down into the axon and the myosin filaments would accumulate in the proximal end of the cell.

With the onset of darkness, relaxation conditions (36) would be established in the cone so that cross-bridges would disengage and filaments could freely glide past one another as the microtubule-dependent elongation process re-extends the cell to its full, dark-adapted length (35).

Evaluation of the Model

The existence of a distal (myoid) half-sarcomere with filaments of appropriate polarity is strongly supported by the observations in this paper. The Z-line equivalent for these filaments is somewhat complex. Filaments of this half-sarcomere arise from dense tips in microvilluslike calyces at the distal end of the cone cell (see Fig. 1). These filaments course the ellipsoid still organized into discrete bundles typical of microvillus core filaments (24) until they reach the myoid where they splay into free filaments presumably capable of interacting with myosin. It seems likely that the ellipsoid filament bundles play cytoskeletal roles similar to those proposed for stiff thin-filament bundles in other cells (13), in addition to acting as anchoring devices for the myoid thin filaments which participate in contraction. A similar type of splayed-bundle phenomenon has been suggested for the microvilli of intestinal epithelial cells (24). In those cells, microvillus core filament bundles splay in the apical cell cytoplasm into individual filaments which are thought to interact with myosin filaments. Decorated microvillus filaments have the same polarity as those described in the cone, with arrowheads pointing away from the distal tips of the microvillus (24). Mooseker (24) suggests that in the brush border the myosin filaments interact with thin filaments from adjacent microvilli and, by pulling these together, move entire microvilli. The model in Fig. 12 proposes a similar mechanism, except that in this case filaments of opposite polarity arise from the proximal (axon) half of the cone rather than from adjacent filament bundles.

The existence of a proximal half-sarcomere in the cone, with distally directed arrowheads, is not so well documented. Because of problems with penetration of S-1 and disruption of structure

during glycerination, it is more difficult to discern the polarities of all filaments in the proximal half-sarcomere (axon) than in the distal myoid (the myoid is bathed directly during incubation, while the axon lies within the osmotically sensitive inner nuclear layer of the retina). Nevertheless, numerous examples have been found of light-adapted cones in which two sets of oppositely directed filaments can be discerned in the axon region (Table I). The high degree of axial alignment, the consistency of polarities in different axons, and the observed increase in percentages of distally directed arrowheads as one proceeds from nucleus to pedicle with a maximum approaching 50% (Table I) together suggest that the filaments with distally directed arrowheads do not arise from random breakage and skewing of the proximally directed filaments or from random polymerization of nonfilamentous actin in the axon by the S-1.

Clearly, though these observations suggest that a proximal set of cone filaments is present, the existence of these filaments is not conclusively demonstrated. Another interpretation is that filaments of both polarities might arise within the axon, so that the distribution of polarities reported in Table I does not represent two separate proximal and distal overlapping sets of filaments. This possibility cannot yet be ruled out.

The model in Fig. 12 predicts that one should see filaments of predominantly one polarity in dark-adapted axons and of both polarities in light-adapted myoids. The reported polarities in light-adapted cones are consistent with this prediction. Unfortunately, the corresponding observations of dark-adapted cones have not been obtainable because these retinas are more severely damaged by glycerination. Further studies of both light- and dark-adapted cones are in progress, using newly developed methods of fixation which provide much clearer arrowheads.

The Z-line equivalent for attachment of the proposed proximal (axon) half-sarcomere is not clear. Because thin filaments are visible in the synaptic region (see Fig. 9), attachment of filaments in this region is feasible. Also, small groups of thick filaments extend into the synapse; these thick filaments are possibly associated with groups of actin filaments which anchor in the synapse and extend into the axon to form the proximal half-sarcomere. Alternatively, filaments may attach to membranes alone the sides of the axons, but because thick filaments accumulate near the syn-

apse in the light and usually retain a central localization in the axon, it seems likely that a majority of the axonal thin filaments extend from the synaptic region. The increasing percentage of filaments with distally directed arrowheads as one proceeds from nucleus toward the pedicle is consistent with this interpretation. Though no specific morphological attachments were seen, the disruption of pedicles by glycerination could obscure any attachment sites.

The distribution of thick filaments in light- and dark-adapted cones is consistent with the predictions of the model in Fig. 12. Thick filaments are predominantly localized in the axon region where most sliding takes place; they are almost always oriented parallel to the long axis of the cone cell, and they accumulate toward the proximal end of the axon in the light. The scattered thick filaments which are occasionally seen in the long myoid of the dark-adapted cone perhaps achieve this position passively as a result of being dragged out by myoid actin filaments during the elongation process. In this region, thick filaments are sometimes randomly rather than paraxially oriented.

The model in Fig. 12 does not necessarily depend on the existence of long myosin thick filaments as illustrated; it merely requires myosin aggregates to be bipolar. If, for example, the axon thick filaments described in this paper are an artifact of fixation and if myosin exists in vivo in a soluble form, the model may still be valid. Smaller myosin aggregates, which nonetheless do deploy myosin molecules in tail-to-tail fashion, could conceivably develop tension as illustrated.

It is consistent with the model in Fig. 12 that in most fish species which exhibit photomechanical movements, the axon is at least as long as the myoid (see Fig. 6 a, 3). Thus, the overlapping of myoid and axon filaments in the light-adapted state is technically feasible. In some species such as the grunt, the myoid shortens from 85 μm to 5 μm in length (9); this extreme (17-fold) shortening of the myoid could be more easily explained by the model in Fig. 12 than by a model in which the mechanism of contraction resides exclusively in the myoid region.

Two observations suggest that contraction is mediated by forces acting along the axial midline of the cone as predicted by Fig. 12. First, the myoid retains relatively constant volume as it contracts (4, 23); thus, the surface area of the myoid is strongly reduced. The membrane and

peripheral cytoplasm of the myoid appear to accommodate this surface reduction passively by assuming flutes and folds which occupy the available space between adjacent photoreceptors. Second, the axial alignment and central aggregation of the thick filaments suggests that they participate in a force developed between opposite ends of the cone cell.

The observed changes in nuclear shape during contraction are consistent with the interpretation that the nucleus is passively deformed and displaced by the filament movements illustrated in Fig. 12. The sliding interdigitation of filaments in the light would produce a net pull on the nucleus toward the pedicle so that the nucleus would tend to move into the axon. During elongation, the disengaging distal thin filaments would tend to drag the nucleus back toward the outer limiting membrane, and also even to deform it into folds where groups of filaments pass from the axon alongside the nucleus toward the myoid. Thick filament groups are often observed within these nuclear indentations.

Alternative explanations of cone contraction based on actomyosin gel shrinkage in the myoid (30) seem unlikely for a number of reasons. The isovolumetric shortening of the cone myoid is inconsistent with a general shrinkage of the myoid cytoplasm, as is the apparently passive folding of the myoid plasma membrane and surface cytoplasm during contraction. Also, the central, paraxial orientation of thin and thick filaments is more consistent with the interpretation that a linear contractile force acts along the axis of the cone cell than with a generalized gel shrinkage. One might expect a more random meshwork of filaments in the gel-shrinkage mechanism (30). Finally, a theory of actomyosin gel contraction in the myoid is inconsistent with the observed localization of thick filaments (presumably myosin) outside the myoid in the cone as myosin is required for such shrinkage (30).

Concluding Remarks

Though the case is not yet complete, the reported structural details of thin and thick filament distribution and polarities of thin filaments in contractile cones of teleosts are consistent with a structural model for cone contraction based on the sliding filament hypothesis for skeletal muscle. It is conceptually appealing that nonmuscle cells and muscle cells should share a common basic mechanism for the contractile process. It is now clear

that nonmuscle contractile proteins have properties very similar to those of muscle proteins, especially with regard to the activating effect of actin on the adenosine triphosphatase activity of myosin and the precise structural form of the actin-myosin complex (29). Because these properties are so directly related to the contractile mechanism in skeletal muscle, it is difficult to believe that such homology would exist in the absence of a common structural basis for contraction.

In the teleost cone, where contraction is recurrent and linear, the contractile apparatus appears to be relatively stable and more highly organized than in cells where contraction is immediately preceded by assembly and followed by disassembly of the contractile apparatus (as it is in most nonmuscle cells). Thus, in the teleost cone the linear contraction, the orderly arrangement of the contractile apparatus, and the absence of assembly and disassembly complications provide a system where underlying contractile mechanisms shared with skeletal muscle may be more easily discerned.

REFERENCES

1. ADELSTEIN, R. S., M. A. CONTI, G. S. JOHNSON, I. PASTAN, and T. D. POLLARD. 1972. Isolation and characterization of myosin from cloned mouse fibroblasts. *Proc. Natl. Acad. Sci. U. S. A.* **69**:3693-3697.

2. ALI, M. A. 1975. Retinomotor responses. *In* Vision in Fishes. M. A. Ali, editor. Plenum Press, New York. 313-355.

3. ALI, M. A., and M. ANCTIL. 1976. Retinas of

Fishes. Springer Verlag, Berlin 365 pp.

4. AREY, L. B. 1916. The movement in visual cells and retinal pigment of the lower vertebrates. *J. Comp. Neural.* **26**:121-201.

5. BEHNKE, O., B. I. KRISTENSEN, and L. E. NIELSEN. 1971. Electron microscopical observations on actinoid and myosinoid filaments in blood platelets. *J. Ultrastruct. Res.* **37**:351-369.

6. BHOWMICK, D. K. 1967. Electron microscopy of *Trichamoeba villosa* and amoeboid movement. *Exp. Cell Res.* **45**:570-589.

7. BOIS, R. M., and D. C. PEASE. 1974. Electron microscopic studies of the state of myosin aggregation in the vertebrate smooth muscle cell. *Anat. Rec.* **180**:465-480.

8. BUCKLEY, I. K. 1974. Subcellular motility: a correlated light and electron microscope using cultured cells. *Tissue Cell.* **6**:1-20.

9. BURNSIDE, B. 1976. Microtubules and actin filaments in teleost visual cone elongation and contraction. *J. Supramol. Struct.* **5**:257-275.

10. BURNSIDE, M. B. 1976. Possible roles of microtubules and actin filaments in retinal pigmented epithelium. *Exp. Eye Res.* **23**:257-275.

11. BURNSIDE, B., and A. M. LATIES. 1976. Actin filaments in apical projections of the primate pigmented epithelial cell. *Inv. Ophthalmol.* **15**:570-575.

12. CLONEY, R. A. 1972. Cytoplasmic filaments and morphogenesis: effects of cytochalasin-B on contractile epidermal cells. *Z. Zellforsch. Mikrosk. Anat.* **132**:167-192.

13. COOKE, R., M. CLARKE, R. J. vonWEDEL, and J. A. SPUDICH. 1976. Supramolecular forms of *Dictyostelium* actin. *In* Cell Motility. Book B., R. Goldman, T. Pollard, and J. Rosenbaum, editor. Cold Spring Harbor Laboratory, Cold Spring Harbor, N. Y. 575-587.

14. COPELAND, D. E. 1974. The anatomy and fine structure of the eye of the teleost. *Exp. Eye Res.* **18**:547-561.

15. GOLDMAN, R., T. POLLARD, J. ROSENBAUM, editors. 1976. *In* Cell Motility. Cold Spring Harbor Laboratory, Cold Spring Harbor, N. Y. 1367 pp.

16. HARTWIG, J., and T. P. STOSSEL. 1976. Interactions of actin, myosin, and an actin-binding protein of rabbit pulmonary macrophages. III. Effects of cytochalasin-B. *J. Cell Biol.* **71**:295-303.

17. HUXLEY, H. E. 1963. Electron microscope studies on the structure of natural and synthetic protein filaments from striated muscle. *J. Mol. Biol.* **7**:281-308.

18. HUXLEY, H. E. 1969. The mechanism of muscular contraction. *Science (Wash. D. C.)* **164**:1356-1366.

19. HUXLEY, H. E. 1973. Muscular contraction and cell motility. *Nature (Lond.).* **243**:445-453.

20. KESSLER, D. 1972. On the localization of myosin in the myxomycete *Physarum polycephalum* and its

possible function in cytoplasmic streaming. *J. Mechanochem. Cell Motility.* **1**:125-137.

21. LOWEY, J., and J. V. SMALL. 1970. The organization of myosin and actin in vertebrate smooth muscle. *Nature (Lond.).* **227**:46-51.

22. MALAWISTA, S. E., J. B. L. GEE, and K. G. BENSCH. 1971. Cytochalasin-B reversibly inhibits phagocytosis: functional, metabolic, ultrastructural effects in human blood leukocytes and rabbit alveolar macrophages. *Yale J. Biol. Med.* **44**:286-300.

23. MILLER, W. H., and A. W. SNYDER. 1972. Optical function in myoids. *Vision Res.* **12**:1841-1848.

24. MOOSEKER, M. 1976. Actin filament-membrane attachment in the microvilli of intestinal epithelial cells. *In* Cell Motility. R. Goldman, T. D. Pollard, and J. Rosenbaum, editors. Cold Spring Harbor Laboratory, Cold Spring Harbor, N. Y. 631-650.

25. NACHMIAS, V. T. 1968. Further electron microscope studies on the fibular organization of the ground cytoplasm of *Chaos chaos*. *J. Cell Biol.* **38**:40-50.

26. PAINTER, R. G., M. SHEETZ, and S. J. SINGER. 1975. Detection and ultrastructural localization of human smooth muscle myosin-like molecules in human non-muscle cells by specific antibodies. *Proc. Natl. Acad. Sci. U. S. A.* **72**:1359-1363.

27. POLLACK, R., M. OSBORN, and K. WEBER. 1975. Patterns of organization of actin and myosin in normal and transformed cultured cells. *Proc. Natl. Acad. Sci. U. S. A.* **72**:994-998.

28. POLLARD, T. D., and S. ITO. 1970. Cytoplasmic filaments of *Amoeba proteus*. *J. Cell Biol.* **46**:267-289.

29. POLLARD, T. D., and R. R. WEIHING. 1974. Actin and myosin and cell movement. *CRC Crit. Rev. Biochem.* **2**:1-65.

30. POLLARD, T. D., K. FUJIWARA, R. NIEDERMAN, and P. MAUPIN-SZAMIER. 1976. Evidence for the role of cytoplasmic actin and myosin in cellular structure and motility. *In* Cell Motility. Book B. R. Goldman, T. Pollard, and J. Rosenbaum, editors. Cold Spring Harbor Laboratory, Cold Spring Harbor N. Y. 689-724.

31. SPOONER, B. S., and N. K. WESSELLS. 1970. Effects of cytochalasin-B upon microfilaments involved in morphogenesis of salivary epithelium. *Proc. Natl. Acad. Sci. U. S. A.* **66**:360-364.

32. TILNEY, L. G., and M. MOOSEKER. 1971. Actin in the brush border of epithelial cells of the chicken intestine. *Proc. Natl. Acad. Sci. U. S. A.* **68**:2611-2615.

33. TILNEY, L. G. 1975. The role of actin in non-muscle cell motility. *In* Molecules and Cell Movement. S. Inoué and R. E. Stephens, editors. Raven Press, New York. 339-388.

34. WALLS, G. L. 1943. The vertebrate eye and its adaptive radiation. Hafner Publishing Co., New York. 785 pp.

35. WARREN, R. H., and B. BURNSIDE. 1978. Microtubules in cone myoid elongation in the teleost retina. *J. Cell Biol.* **78**:247–259.

36. WEBER, A. M., and J. M. MURRAY. 1973. Muscular control mechanisms in muscle contraction. *Physiol. Rev.* **53**:612–671.

37. WEBER, K., and U. GROESCHEL-STEWART. 1974. Antibody to myosin: the specific visualization of myosin-containing filaments in non-muscle cells. *Proc. Natl. Acad. Sci. U. S. A.* **71**:4561–4564.

38. WEIHING, R. R. 1976. Cytochalasin-B inhibits actin-related gelation of HeLa cell extracts. *J. Cell Biol.* **71**:303–307.

39. WRENN, J. T., and N. K. WESSELLS. 1970. Cytochalasin-B: effects upon microfilaments involved in morphogenesis of estrogen induced glands of oviduct. *Proc. Natl. Acad. Sci. U. S. A.* **66**:904–908.

40. ZUCKER-FRANKLIN, D. 1969. Microfibrils of blood platelets: their relationship to microtubules and the contractile protein. *J. Clin. Invest.* **48**:165–175.